Modelling and Simulation in Materials Science and Engineering 27 (2019) 085015 (17 pages).

Size Effect in Molecular Dynamics Simulation of Nucleation Process during Solidification of Pure Metals: Investigating Modified Embedded Atom Method Interatomic Potentials

Avik Mahata[a] and Mohsen Asle Zaeem[a,b*]

[a] Department of Materials Science and Engineering, Missouri University of Science and Technology, Rolla, MO 65409, USA

[b] Department of Mechanical Engineering, Colorado School of Mines, CO 80401, USA

Abstract:

Due to the significant increase in computing power in recent years, the simulation size of atomistic methods for studying the nucleation process during solidification has been gradually increased, even to billion atom simulations (sub-micron length scale). But the question is how big of a model is required for size-independent and accurate simulations of the nucleation process during solidification? In this work, molecular dynamics simulations with model sizes ranging from ~2,000 to ~8 million atoms were used to study nucleation during solidification. To draw general conclusions independent of crystal structures, the most advanced second nearest-neighbor modified embedded atom method interatomic potentials for Al (face-centered cubic), Fe (body-centered cubic), and Mg (hexagonal-close packed) were utilized for molecular dynamics simulations. We have analyzed several quantitative characteristics such as nucleation time, density of nuclei, nucleation rate, self-diffusion coefficient, and change in free energy during solidification. The results showed that by increasing the model size to about two million atoms, the simulations and measurable quantities become entirely independent of simulation cell size. The prediction of cell size required for size-independent computed data can considerably reduce the computational costs of atomistic simulations and at the same time increase the accuracy and reliability of the computational data.

Keywords: Size effect; Nucleation; Solidification; Molecular dynamics; MEAM; Metals.

*Corresponding author; email: zaeem@mines.edu (M. Asle Zaeem)

1. Introduction

Solidification and crystallization by nucleation is very common in manufacturing processes of different materials, including metals and alloys. The major challenge in experimental observation of nucleation is that the entire process of nuclei formation and growth happens in the interior part of the liquid metals. Therefore it is beneficial to use theoretical or computational tools such as classical nucleation theory (CNT) [1, 2], density function theory (DFT) [3], molecular dynamics (MD) [4-6], Monte Carlo (MC) [7, 8], phase-field [9-13], and cellular automaton [14, 15] to study solidification and nucleation phenomena. Theoretical tools such as CNT do not predict the dependability on system size, as the probability of forming crystal nuclei is per unit time and unit volume and is related to the free energy barrier for formation of the critical nucleus [16]. On the other hand, even the most advanced and hybrid MC simulations are limited to very small number of atoms [17, 18], whereas phase-field or cellular automaton models are applied in a considerably larger length scales and unable to study the nucleation process in details [19, 20]. Among the mentioned methods, MD simulations have the flexibility to cover length scales between sub-nanometer to sub-micrometer scales depending on the computing resources, and they seem to be the suitable computational method to study the nucleation process.

MD simulations have been used to study the nucleation process in different metals and alloys at different length scales [21-23]. However, it is a well-established fact that the accuracy of MD simulations depends on the utilized interatomic potentials. In the literature, the nucleation process during solidification has been studied for model sizes ranging from a few thousand atoms [24, 25] to million [6, 25] and billion atoms [26]. However, by increasing the model size the accuracy of the predictions is not necessarily improved. For example, the Finnis–Sinclair (FS) interatomic potential used for the billion atom MD simulation of pure Fe solidification [26] predicts the meting temperature to be 2,400 K, which is ~600 K higher than the physical melting temperature of Fe. On the other hand, the simulation size can influence the results, and it is customary to use larger simulation boxes to circumvent simulation size effects. There has been some disagreements on how large the simulation size should be for a reliable study of nucleation [22, 27], however the expectation has always been that a sufficiently large simulation cell would resolve the issues related to finite size effect.

Size effect in MD simulations was studied by Streitz et al. [22] who predicted at least 8 million (M) atoms are required for size-independent MD models when utilizing many-body, angular-dependent interaction potentials; it should be mentioned that this interatomic potentials were not explicitly fitted to solid-liquid coexistence properties (e.g., melting point). The other studies were done by utilizing Lennard-Jones [28-30] and hard-sphere model [31] potentials, which are also very simple interatomic potential models and incapable of predicting high temperature properties. The studies completed based on the Lennard-Jones interatomic potential were also limited to simulation size of about 4,000 atoms [29, 30]. Embedded Atom Methods (EAM) which is very similar to FS interatomic potentials predicts relatively accurate solid-liquid coexistence for several metallic system [32-34]. However, the most recent studies of solid-liquid coexistence of metallic systems utilizing EAM potentials were also limited to much smaller length scale [34]. EAM was further modified (MEAM) to include the directionality of bonding in covalent materials in the EAM formalism [35]. Today, the MEAM potentials are widely used in the computational materials science and engineering community to simulate unary, binary, ternary and multi-component metallic systems with microstructural features, such as grain boundaries, defects, free surfaces, etc.

As the interatomic potential becomes more accurate to predict solid-liquid coexistence properties, it becomes more expensive computationally [36]. Thus, it is important to determine the optimum model size for simulating the nucleation process by MD simulations in order to be scientifically accurate without any finite size effects. In recent literature, there are a few theoretical, computational and experimental studies which investigated the size effect in crystal nucleation [37-39]. They studied various aspects of nucleation such as free energy change, nucleation rate, and solid-liquid coexistence properties, but they did not provide enough details about an optimum finite size that can be used in general to get accurate insights about the nucleation process during solidification of different material systems.

To address the issues related to the finite size effect of atomistic simulations, we performed MD simulations ranging from a few thousand atoms to several million atoms utilizing the most advanced second nearest-neighbor MEAM (2NN-MEAM) interatomic potentials to predict an optimum simulation size for nucleation studies. We performed computations for three different metals, Al with face-centered cubic (fcc), Fe with body-centered cubic (bcc) and Mg with

hexagonal-close packed (HCP) crystal structures to ensure that the results can be extended to other metallic systems with different crystal structures. Isothermal solidification is used in all the simulation, and we quantified the nuclei size, density, diffusivity, free energy and also nucleation rate for different model sizes in order to identify the size-independent models.

2. Simulation Methodology

2.1 Simulation models

We built MD simulation models using 10 different box sizes, ranging from 2,000 to 8 M atoms. Solidification temperatures was chosen between 300 K and 750 K for Al, between 800 K and 1,250 K for Fe, and between 300 K and 700 K for Mg, with 50 K intervals. Therefore total of 10 solidification temperatures were tested for MD simulations of each of the studied metals. Each simulation was repeated 5 times with slightly different initial velocity of atoms to determine the statistical errors. Total of 1,500 MD simulations were estimated (3 materials x 10 temperatures x 10 model sizes x 5 times) to complete the study. However, below a specific cell size and above a specific temperature (see section 3.2, Table 3), the nucleation doesn't occur under any conditions. Therefore about 1,000 simulation runs were sufficient to complete the study on size effect. The details of various simulations that we performed are given in Table 1. As the lattice constants (Al, Fe and Mg are 4.05 Å, 2.86 Å, and 3.20 Å, respectively) and crystal structures are different, the total number of atoms are not exactly same for the same size supercells of these three metals. We used isothermal-isobaric (NPT) ensemble and a time step size of 0.003 ps for all simulations. Nucleation by solidification occurs within the first 300 ps of simulation for most of the cases. For cases that nucleation does not appear, the maximum time used for those simulations is 3,000 ps (1,000,000 time steps). Temperature was controlled by Nose-Hoover thermostat and pressure was stabilized by Parrinello-Rahman barostat [40]. LAMMPS [41] code and OVITO [42] were used for the MD simulations and visualization of nucleation and solidification processes, respectively. Within OVITO, common neighbor analysis algorithm (CNA) was used [43] to identify the local structures of atoms. The cut-off used for CNA is ~80% of the lattice constants of Al and Fe to identify the fcc and bcc clusters. As Mg has a c/a ratio of 1.625 for its hcp crystal structure, we used the cut-off of 4.16 Å (c≈5.20 Å). MATLAB was used to solve equations numerically [44].

Table 1. The initial simulation set up for the MD simulation of solidification of Al, Fe and Mg.

Element	Unit Cells	Cell Size (nm^3)	Atoms (approx.)	Temperature Range (K)
Al	10-160	2.86-45.80	2,000-8,000,000	300-750
Fe	10-125	4.05-50.70	4,000-8,000,000	700-1,250
Mg	10-178	5.0-55.39	5,000-8,000,000	300-700

2.2 Interatomic potential

There are several interatomic potentials in the literature that have been used to study solidification of metallic systems. Many body interatomic potentials such as Finnis–Sinclair (FS) [45, 46] and Embedded Atom Method (EAM) [47] have been extensively used for solidification studies [6, 48-50]. However, both FS and EAM potentials fail to predict the melting point or the solid-liquid coexistence properties accurately for the most metallic systems. Extended FS potentials were studied for solidification of various metals such as Fe, Mo, Ta, and W by Dai et al. [51], which showed between 200 and 500 K discrepancies between MD predictions and experimental data for the melting points of these metals. On the other hand semi-empirical many body EAM potentials has been used for solid-liquid coexistence more often [47, 52] and predict the melting point properties more accurately [53]. In this work, we are utilizing the 2NN-MEAM potentials, which are the most accurate interatomic potentials for high and low temperature properties of metals. The detailed comparison of both low and high temperature experimental properties and those calculated by MD simulations utilizing 2NN-MEAM potentials [48-50, 54] are given in Table 2.

Table 2. Properties of Al, Fe and Mg predicted by MD simulations utilizing the 2NN MEAM interatomic potential and experimental results.

	Al		**Fe**		**Mg**	
Properties	Experiments	MEAM MD [48]	Experiments	MEAM MD [49]	Experiments	MEAM MD [50]
Bulk Modulus (GPa)	76.4[a]	79.4	167[e]	166	36.9 [a]	36.9
C_{11} (GPa)	111.5[a]	114.3	230[e]	231	63.5[a]	62.9
C_{12} (GPa)	58.8[a]	61.9	135[e]	134	18.8[a]	18.4
C_{44} (GPa)	29.5[a]	31.6	117[e]	116	1.84 [a]	1.71
Specific Heat (J mol^{-1} K^{-1})	26.15[b]	24.70	25.50[e]	26.18	25.9[f]	25.6
Thermal Expansion Coeff. (10^6 K^{-1})	17.31[b]	23.50	12.10[e]	11.80	26[f]	27.8
Melting Point (T_m) (K)	934[c]	925	1811[e]	1807	937.9[f]	923.2
Solid–liquid interface free energy (mJ/m^2)	168.9±21 to 158±30[d]	172.6	184[e]	188	122.2[g]	90.0

[a] [55] , [b] [56], [c] [56-58], [d] [59-61], [e] [62-65], [f] [66], [g] [33]

3. Results and Discussions

3.1 Visualization of Nucleation

Fig. 1(a-l) shows the nucleation for Al, Fe, and Mg in an intermediate stage before the solid nuclei have grown enough to merge and form grain boundaries. The Al in the display (Fig. 1(a-d)) was solidified at 500 K, Fe (Fig. 1(e-h)) at 1,100 K, and Mg (Fig. 1(i-l)) at 600 K. The process of solidification by nucleation is random and the solidification can start from any parts of the simulation box. In Al solidification, the nucleation happens primarily by formation of fcc (green) atoms (Fig. 1(a-d)) and it also accompanied by some solidification defects, which can be identified as hcp stacking faults, as shown in details in Mahata et al. [6]. The Fe and Mg nucleate by

formation of bcc (blue) atoms (Fig. 1(e-h)) and hcp (red) atoms (Fig. 1(i-l)), respectively. It is clear from Fig. 1 that the system size for MD simulations needs to be large enough to support the formation and growth of one or multiple critical nuclei. It is important to point out that this system-size dependence is due to the increased probability of forming a critical nucleus when the system size is larger, and it is not an artifact due to the periodic boundary conditions.

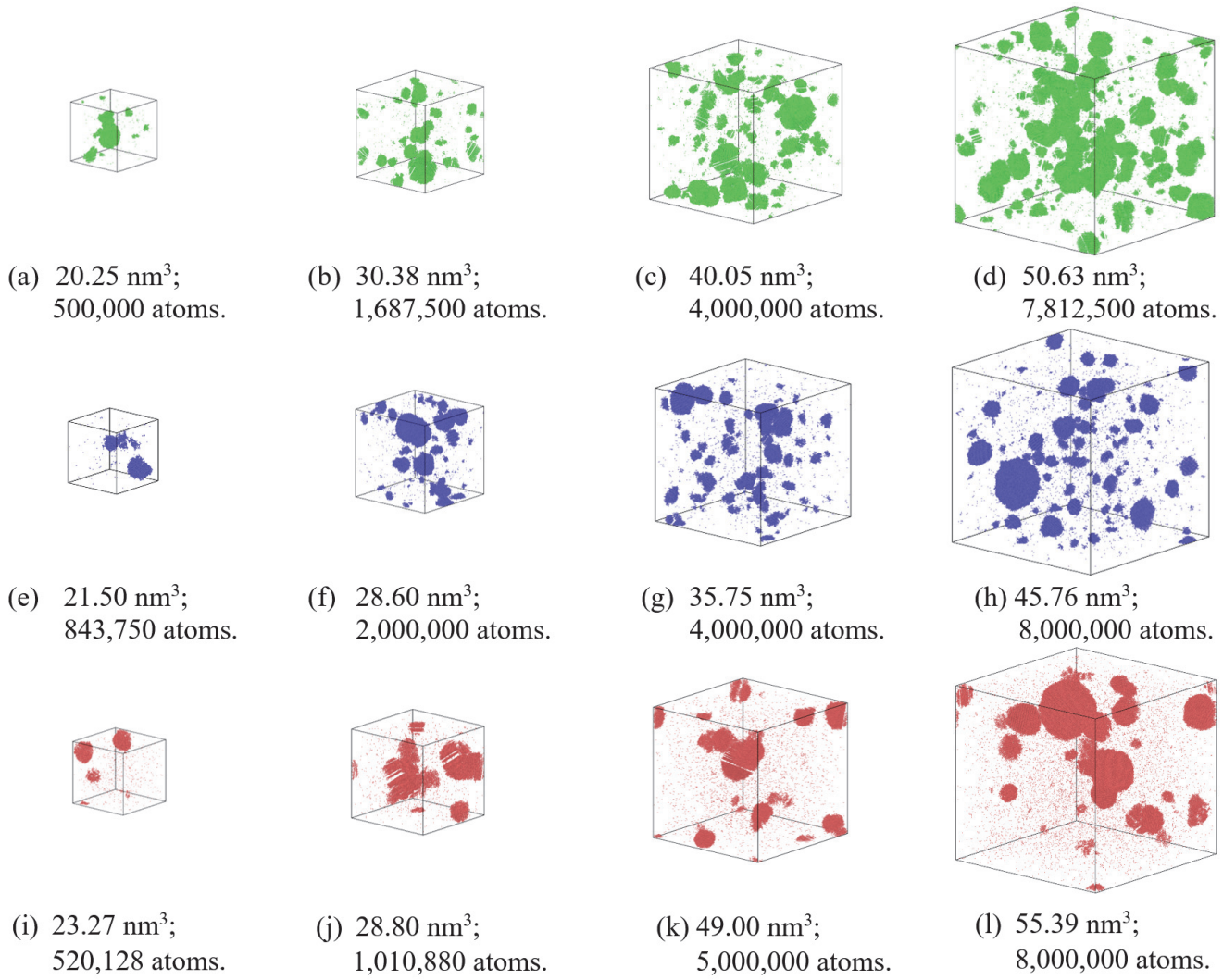

Fig. 1. Nucleation during isothermal solidification in different simulation sizes: (a-d) Al at 500 K, (e-h) Fe at 1100 K, and (i-l) Mg at 600 K. The green atoms represent the fcc atoms, blue atoms represents the bcc atoms, and red atoms represent the HCP atoms. This figure only shows the primary crystalline phase, and hcp atoms in Al, ico atoms in Fe, fcc atoms in Mg, and the liquid atoms in all the cases are not shown for better visualization of the nuclei.

3.2 Size effect criteria in MD simulations

Both the solidification temperature and simulation size influence the solidification process in MD simulations. Temperature is always the primary factor that impacts the solidification, and beyond a threshold temperature range the simulation box cannot be solidified for any box sizes in MD simulations. For example, above 725 K, the Al atoms cannot be solidified regardless of the simulation cell size [6]. In the same way, there is no solidification observed above 700 K for Mg and 1,250 K for Fe in MD simulations. This limitation of nucleation temperature is specifically applied to the observation in MD simulation due to its time and length scales. In theory, the solidification by nucleation in metallic system is possible at any temperatures lower than the melting temperatures. Although the temperature is the primary governing factors in solidification by nucleation, in MD simulations the length and time scale is also prohibits the nucleation from happening. For a smaller size simulation box, the number of atoms are considerably low and there might not be enough atoms to form critical nucleus. In our previous study [6] we showed that the critical nucleus in Al is consisted of 1,000-2,000 atoms and its average size is 4-5 nm in diameter. In Fig. 2, we present formation of a critical nucleus during nucleation from liquid Mg. The critical nuclei is one of the most impotent part of studying solidification as it initiates the solidification process. The critical nucleus in Mg consists of ~1,500 atoms in a 1M atom simulation box. Depending on the system size we can study the formation of the multiple nuclei formation. The typical size critical nuclei with 1,000-2,000 atoms are a significant faction of the total number of atoms in a smaller size box. In a nucleation process where the nuclei form by random fluctuation of a very small number of atoms, it is very unlikely that atoms stabilize to form crystalline solid structures.

Along with the length scale, time is also a constrain for MD simulation which prohibits solidification at very low undercooling. The time-temperature-transformation (TTT) diagram for any materials [67] suggests that the time required for solidification gradually increases with decreasing undercooling. In our previous studies on nucleation of Al [6], we plotted a similar TTT curve considering the time required to crystallize at least 40% of atoms from undercooled liquid Al, and we showed a dramatic increase in time for isothermal solidification at 725 K for sample size of 1M atoms. In the later stages of the article in Fig. 4, we discuss the induction/incubation time required for the nucleation to start. It shows more time required for solidification to start in

smaller simulation size. So, with both increasing temperature and decreasing size the nucleation and solidification may not occur for certain temperatures and simulation sizes in MD simulations.

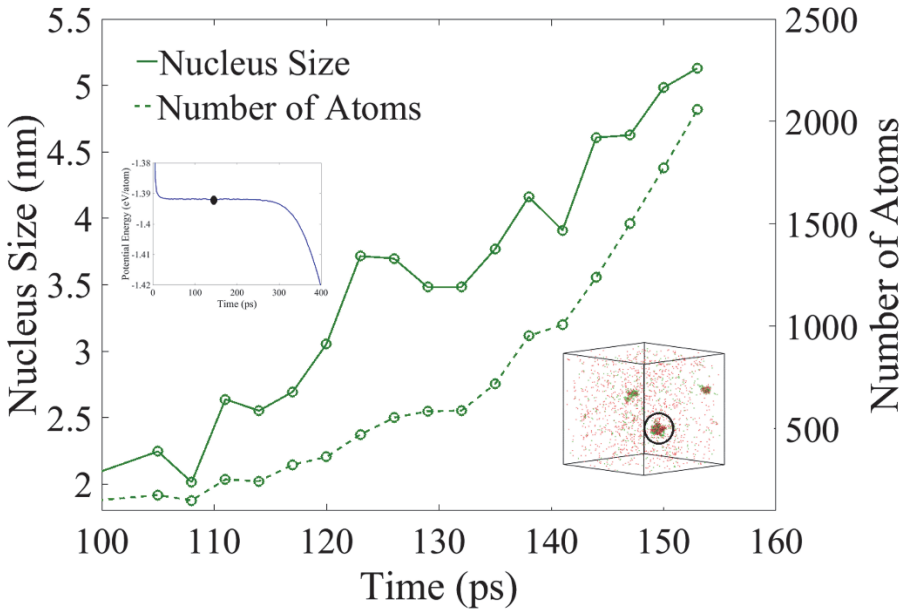

Fig. 2. Formation of the first critical nucleus inside the Mg melt at 600 K isothermal solidification. Inset on top shows the decreasing potential energy with time. The bottom inset shows the critical nucleus inside a simulation box with ~1M atoms.

Table 3 shows for isothermal solidification of Al at 450 K and 500 K, a simulation box with only 24,000 atoms was required to observe nucleation and solidification, whereas a minimum of 62,500 atoms was required to form a critical nucleus at 700 K. The similar characteristic applies for Fe and Mg, and the minimum number of atoms in the simulation box to observe nucleation varies by the isothermal solidification temperature. The nucleation happens optimally (i.e., critical nucleation temperature) between a temperature range of 400 K and 500 K for Al, between 1,000 K and 1,100 K for Fe, and between 500 K and 600K for Mg. In the case of Al, at lower solidification temperatures (or higher undercooling) such as 300 K or 400 K, the solidification will occur but crystal nucleation is rare. As shown in our previous work on Al [6] and Fe [68], a high undercooling results in formation of a glassy solid. Therefore, the temperature-dependent size effect should be considered in MD simulations of the crystal nucleation process.

Table 3. Minimum simulation size (number of atoms in the simulation box) to observe nucleation during solidification at different temperatures for Al, Fe and Mg.

Element	Temperature	Minimum Size	Element	Temperature	Minimum Size	Element	Temperature	Minimum Size
Al	400	62,500	Fe	800	128,000	Mg	350	268,192
	450	24,000		850	128,000		400	111,800
	500	24,000		900	128,000		450	21,840
	550	24,000		950	128,000		500	10,032
	600	62,500		1,000	54,000		550	10,032
	650	62,500		1,050	54,000		600	21,840
	700	62,500		1,100	31,250		650	111,800
	725	108,000		1,200	128,000		700	111,800

In order to understand the effects of the mobility of atoms on nucleation process from an under-cooled melt, the self-diffusion coefficients of the undercooled Al, Fe and Mg melts were estimated from the mean-square displacement (MSD) analysis. The MSD can be defined as the squared difference of current and initial positions of atoms, $|r_i(t) - r_i(0)|^2$, where $r_i(t)$ and $r_i(0)$ are the position of atom i at time t and 0, respectively [69]. The self-diffusion coefficient can be estimated from Einstein's relation [70], which is the slope of the MSD versus time divided by six, $\lim_{t\to\infty} \frac{1}{6t}|r_i(t) - r_i(0)|^2$.

As shown in Fig. 3(a-c), the self-diffusion coefficient fluctuates when the simulation size is very small (typically a simulation box with less than 20,000 atoms). It was also reported previously that the diffusivity generally fluctuates in simulations with smaller box sizes and tend to be more stable in larger size simulations [71-73]. By increasing the simulation size to more than 1 M atoms, the self-diffusion stabilizes and converges to the value of the simulation with the largest size box (~8 M atoms) that we tested. This suggests that a million-atom simulation can be the optimum simulation size for MD simulation of solidification. Fig. 3 also suggests that for large enough simulation boxes, temperature is the primary factor in solidification, as the diffusion coefficient increases with increasing the solidification temperature. At very high undercoolings or very low isothermal solidification temperatures, the solidification happens very fast due to higher differences in mobility of high and low temperature atoms. The melt solidifies extremely fast and

a glassy solid is formed with a very few solid nuclei [6, 68]. When the solidification temperature is too high (or at very low undercooling temperatures), the atoms have a higher mobility; the atoms remain liquid for solidification temperatures higher than 725 K (0.77 T_m) for Al, 1,200 K (0.69 T_m) for Fe, and 700 K (0.75 T_m) for Mg in MD simulations. As the simulation temperature approaches these threshold limits for nucleation, the excessive thermal vibration and self-diffusivity makes it difficult to form solid nuclei. As suggested in Fig. 2, the simulation size at a specific temperature has to be in an optimum range to observe the nucleation process. In Table 3, we present the minimum simulation size to observe nucleation at different isothermal temperatures. Increasing the simulation size will guarantee the nucleation to happen as the diffusivity becomes almost constant with increasing the box size. But there is always a minimum simulation size to stabilize the mobility or the thermal vibration in the atoms to form stable solid crystals.

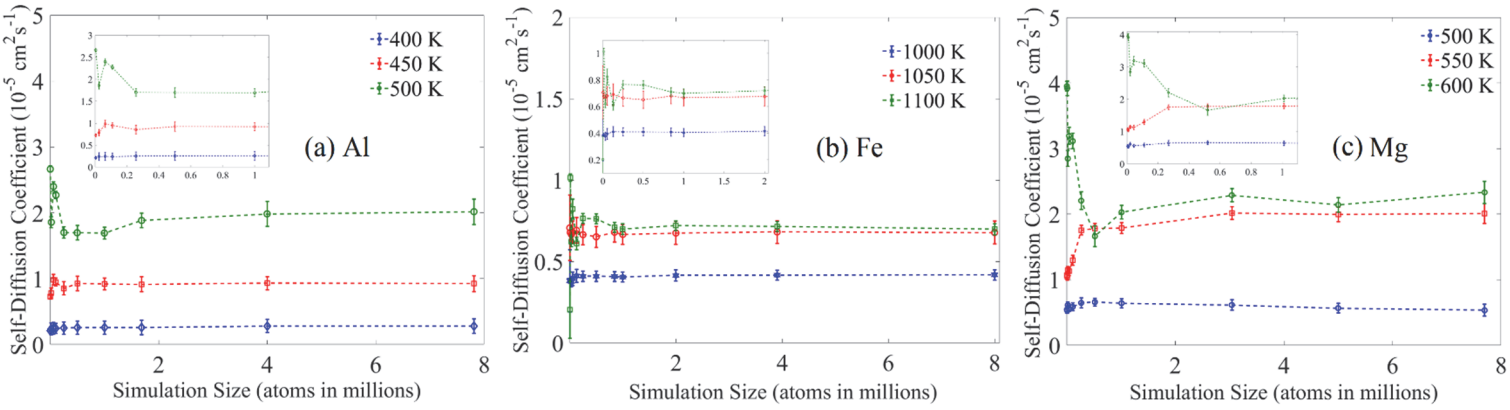

Fig. 3. Self-Diffusion coefficient for different simulation sizes for (a) Al, (b) Fe, and (c) Mg. The errors were calculated using 5 different simulations for each case.

3.3 Size effect on critical nuclei formation and nucleation density

By increasing the simulation size, the overall number of nuclei increases before the start of coarsening or grain boundary formation. The maximum number of separable critical nuclei per unit volume (nuclei density) is plotted as a function of the simulation size in Fig. 4(a-c). The smallest simulations considered for Al, Fe and Mg had 4,000, 2,000 and 5,000 atoms, respectively, where no nuclei formation happened. For all three metals, when the number of atoms in simulation box is less than 2M atoms, nuclei density varies significantly by changing the box size. For

example in the case of isothermal solidification of Al at 500K, when simulation boxes have between 25,000 and 2,000,000 atoms, the nuclei density varies between 1.5 and 2.6x10^{-3} per nm^3 (Fig. 4(a)). The nuclei density drops and shows less fluctuation for larger simulations with more than 2M atoms. For systems larger than 2M atoms, the nuclei density for Fe and Mg remains unchanged with an error margin of 0.20x10^{-3} per nm^3.

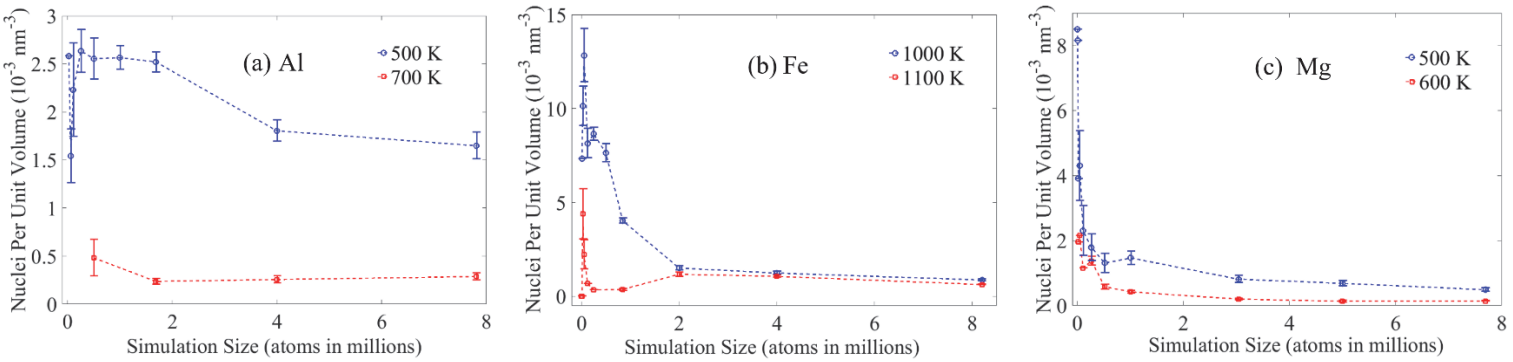

Fig. 4. The increasing number of critical nuclei with increasing cell size shown for (a) Al, (b) Fe and (c) Mg at different temperatures.

We also illustrate the variation of incubation time versus the system size in Fig 5. The incubation time is referred to the time taken by the liquid metal to form the first critical solid nucleus. This can be also referred to as induction time or nucleation time. The nucleation time for the smaller simulation size is much longer than simulations with 2M-8M atoms for both Al and Fe. The nucleation time goes down with increasing the box size. This happens due to increasing the probability of forming critical nuclei in bigger simulation boxes. The results demonstrate that in order to obtain accurate simulated nucleation times, the system size used must be large enough to support the growth of multiple critical nuclei within less timescale. Solidification simulation with 2M atoms can reduce the required time for the study nucleation phenomena by a large margin.

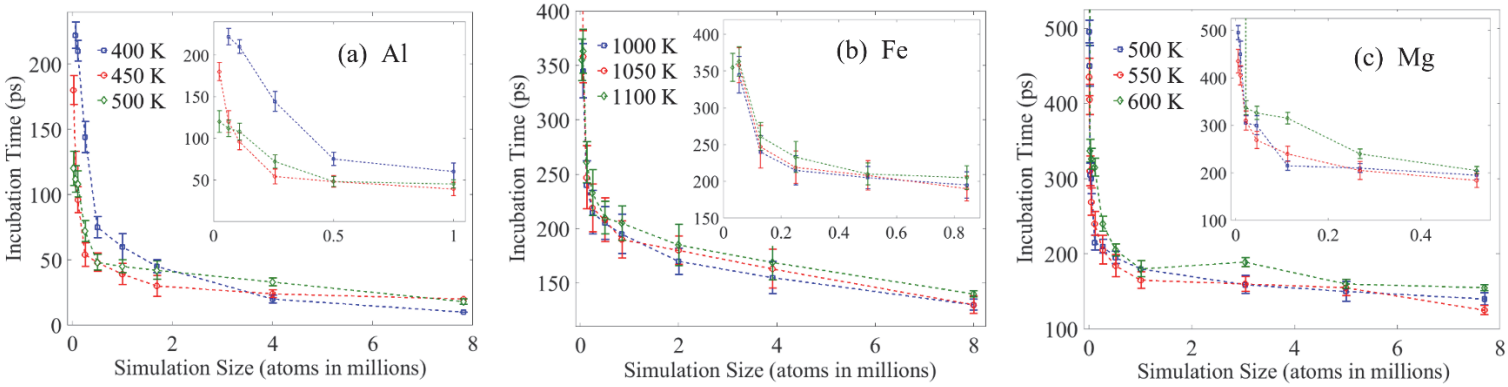

Fig. 5. The formation time for the first critical nucleus is calculated for (a) Al and (b) Fe and (c) Mg for different temperatures and system sizes.

The size of nuclei before coarsening (nano/microstructure formation) increases by increasing the cell size until reaching a threshold (Fig. 6). This size effect is very significant at smaller size simulations up to 1M atoms for all three metals, and the maximum nuclei size increases almost linearly by increasing the cell size up to 1M atoms. However, when the simulation has at least 1.5M to 2M atoms, the maximum size of nuclei remain almost constant. By increasing the simulation size beyond 2M atoms the number of critical nuclei per unit volume (nuclei density) remains almost the same, this is why the maximum nuclei size before start of coursing remains almost constant.

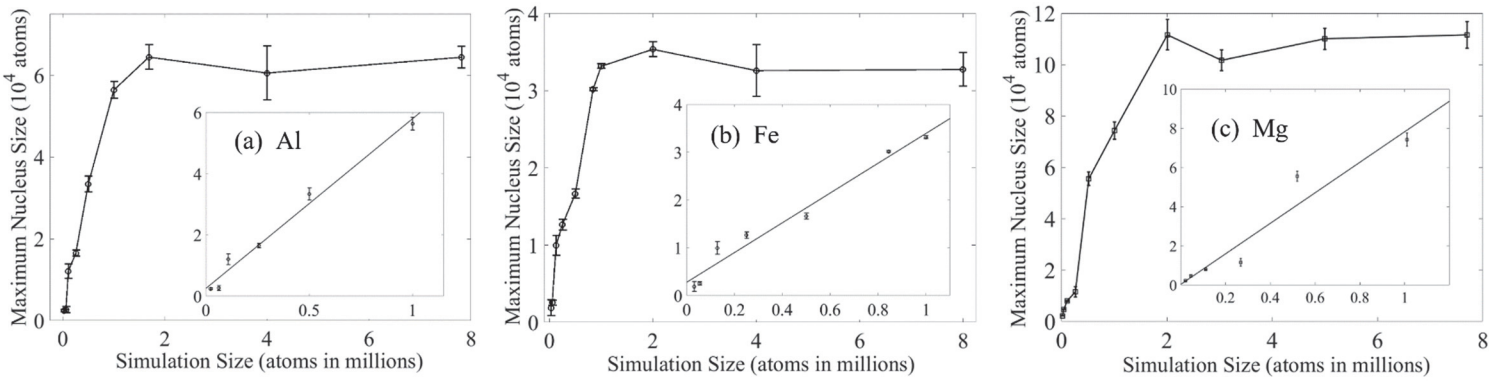

Fig. 6. The maximum nuclei size is shown for (a) Al at 500 K, (b) Fe at 1100 K, (c) Mg at 600 K for different simulation sizes.

3.3 Size effect on free energy and nucleation rate

The free energy landscape during solidification by nucleation can be described by the mean first-passage time (MFPT) method [74, 75]. The MFPT is defined as the average elapsed time for a system that crosses the activated barrier to another steady state for the first time. When the system reaches a transition state (in our case, liquid to solid transition), it is thought that the free energy barrier climbs its top and the system has a 50% probability of stepping into a new steady state. So, the MFPT (or time), solid atom fraction and the free energy are interrelated quantities, and the dynamics of various nonequilibrium and activated process can be described by Fokker-Plank equation [76],

$$\frac{\partial P(x,t)}{\partial t} = \frac{\partial}{\partial x}\left[D(x)e^{-\beta\Delta G(x)} \frac{\partial}{\partial x}(P(x,t)e^{\beta\Delta G(x)} \right] = -\frac{\partial J(x,t)}{\partial x}. \quad (1)$$

Where x is the number of particles (or atoms) in the system, $P(x,t)$ is the probability density that the number of particles (or atoms) in the system is x at time t. $J(x,t)$ can be referred to the nucleation rate in our case, and $D(x)$ is the diffusion coefficient. $\Delta G(x)$ is referred to the free energy landscape, and $\beta = 1/k_B T$, where T is the temperature and k_B is the Boltzmann's constant. When the system is in steady state, the probability density $P_{st}(x)$ becomes time independent, $\frac{\partial P_{st}}{\partial t} = -\frac{\partial J}{\partial t} = 0$, and thus Eq. (1) yields to,

$$\frac{\partial(\beta\Delta G(x))}{\partial x} = -\frac{\partial \ln P_{st}(x)}{\partial x} - \frac{J(x,t)}{D(x)P_{st}(x)}. \quad (2)$$

By integrating Eq. (2), we get,

$$\beta\Delta G(x) = \ln[B(x)] - \int \frac{dx'}{B(x')} + C. \quad (3)$$

$B(x)$ can be evaluated by,

$$B(x) = \frac{1}{P_{st}(x)}\left[\int_{a}^{x} P_{st}(x')dx' - \frac{\tau(x)}{\tau(b)}\right]. \quad (4)$$

$\tau(x)$ is any time before the formation of the maximum size cluster or coarsening, and $\tau(b)$ is the time required for coarsening. The original MFTP method was applied to only a very small simulation sizes in MD (200-1000 atoms). The quantities and the computations for the MFTP and the free energy have been modified according to the large scale systems like the modern MD simulations [38, 77, 78]. In our case of liquid to solid transformation, the maximum nucleus size occurs exactly when the coarsening starts. The probability ($P_{st}(x)$) of finding the maximum size solid cluster (or nucleus) is reciprocal of the total number of nuclei. For a large box size, the coarsening can be identified but there can be multiple maximum size clusters. The size and shape of the nuclei are weakly defined and they hardly take a perfectly spherical shape. At the same time, it is fairly simple to compute the fraction of crystalline atoms in the system, noting that the crystallization time varies by changing the simulation size. To form the crystalline nuclei, each of the crystalline atoms have to overcome the free energy barrier. Therefore, identifying the crystalline atoms and determining the nucleation time can help us compute the free energy landscape.

In our case, the probability is the solid fraction for estimating the free energy landscape ($\beta\Delta G(x)$). The solid fractions in the liquid Al, Fe and Mg have been estimated by averaging over five different simulations with different initial conditions. Then we applied standard discretization method to numerically evaluate Eq. (4), and we get similar free energy landscapes described by Wedekind et al. [28, 75]. The $\beta\Delta G(x)$ generally goes down monotonically as the isothermal solidification temperature of 500 K for Al guarantees the nucleation to happens. However, as the sample size is changing the time required for coarsening or the formation of the maximum size cluster is changing, and also the fraction of atoms in nuclei before the coarsening changes. In this way, we can estimate the change in free energy before formation of the maximum nucleus size or coarsening. In the same way, we also repeat the same procedure for Fe at 1100 K and Mg at 600 K to obtain the change in free energy for these elements.

As shown in Fig. 7, the change in free energy starts at higher values for smaller simulations and gradually decreases to a constant value as the simulation size increases to about 1M atoms. This observation suggests that the simulation becomes size independent when the system size is larger than 1M atoms for any metallic system.

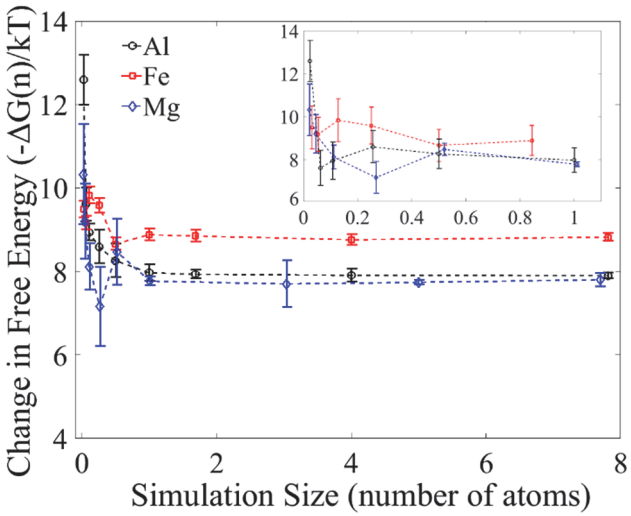

Fig. 7. The change in free energy $\left(-\Delta G(x)/k_B T\right)$ in isothermal solidification of Al (500 K), Fe (1100 K) and Mg (600K) for different simulation sizes.

We also calculated the nucleation rate for each annealing temperature by fitting a straight line to the data on number of nuclei versus time, where the slope of the line is the nucleation rate [6]. Nucleation rate does not show any significant change for system sizes larger than 1M atoms for Al, 500,000 atoms for Fe, and 1M atoms for Mg (Fig. 8(a-c)). The size effect is shown for smaller simulation sizes in the inset of Fig. 8, and it almost linearly increases with increasing the simulation size.

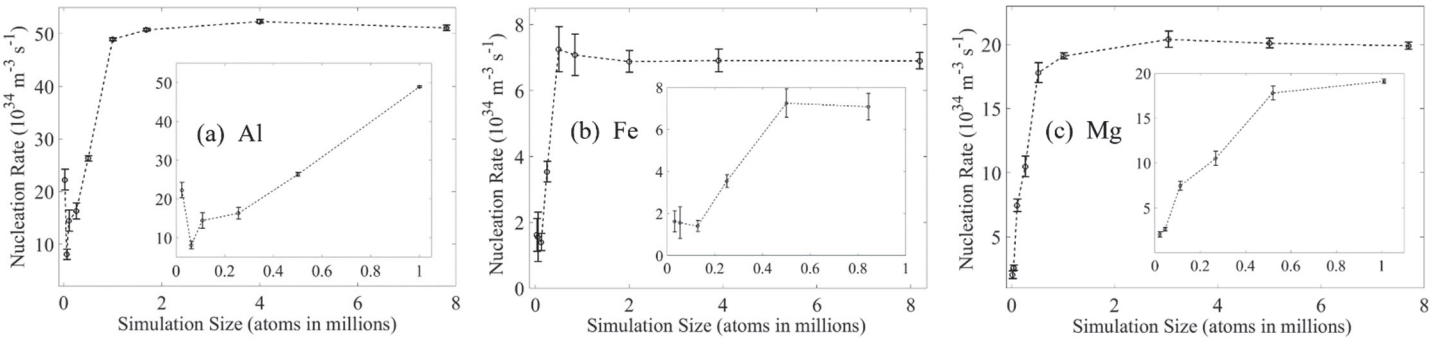

Fig. 8. The nucleation rate for different simulation size is shown for (a) Al at 500 K, (b) Fe at 1,100 K, (c) Mg at 600 K.

4. Conclusion

We presented the results of large-scale atomistic simulations of solidification of molten metals, and studied the effect of simulation size at different isothermal solidification temperatures. To draw general conclusions independent of crystal structures, the most advanced 2NN-MEAM interatomic potentials for Al (face-centered cubic), Fe (body-centered cubic), and Mg (hexagonal-close packed) were utilized for MD simulations.

The temperature of solidification is the most important factor in determining the optimum simulation size. At higher temperatures, the mobility of the atoms increases due to increase of kinetic energy of system. At much lower temperatures (such as 300 K) when the undercooling is very high, the solidification occurs suddenly by freezing of liquid atoms into glassy amorphous solid. However, this phenomenon is not a part of solidification by crystal nucleation. The mobility of the atoms remains in an optimum level for nucleation between 400-500 K for Al, 1000-1100 K for Fe, and 500-600 K for Mg, and the self-diffusion coefficient remains size-independent for simulations with more than 1M atoms. Similarly, change in free energy and nucleation rate remain size-independent for simulations with more than 1M atoms. However, for most cases, the nuclei density and the maximum nuclei size show simulation size dependency up to 2M atom simulations.

The instability of the nucleation process for larger simulation sizes can be also attributed to the periodic boundaries. The percentage of atoms interacting at the boundaries is significant at smaller simulation boxes, but by increasing the simulation size the ratio of number of atoms at the boundaries to those of the bulk decreases significantly, and the number of nuclei that interacts at

the periodic boundaries becomes negligible compared to the total number of nuclei available at any time during the solidification.

Based on our results, we conclude that for MD simulations of nucleation during solidification about 2M atoms is sufficient for simulating a size-independent nucleation phenomena under the condition that the interatomic potential is verified in details for melting and solid-liquid coexistence.

Acknowledgments

Authors would like to acknowledge the funding support from the U.S. National Science Foundation (grant numbers: CMMI 1537170 and CMMI 1855491). Authors are grateful for the computer time allocation provided by the Extreme Science and Engineering Discovery Environment (XSEDE), award number TG-DMR140008.

References

[1] G. Neilson, M. Weinberg, A test of classical nucleation theory: crystal nucleation of lithium disilicate glass, Journal of Non-Crystalline Solids, 34 (1979) 137-147.
[2] D. Erdemir, A.Y. Lee, A.S. Myerson, Nucleation of crystals from solution: classical and two-step models, Accounts of chemical research, 42 (2009) 621-629.
[3] G. Kahl, H. Löwen, Classical density functional theory: an ideal tool to study heterogeneous crystal nucleation, Journal of Physics: Condensed Matter, 21 (2009) 464101.
[4] S. Toxvaerd, Molecular-dynamics simulation of homogeneous nucleation in the vapor phase, The Journal of Chemical Physics, 115 (2001) 8913-8920.
[5] X. Sui, Y. Cheng, N. Zhou, B. Tang, L. Zhou, Molecular dynamics simulation of solidification process of multicrystalline silicon from homogeneous nucleation to grain coarsening, CrystEngComm, (2018).
[6] A. Mahata, M. Asle Zaeem, M.I. Baskes, Understanding homogeneous nucleation in solidification of aluminum by molecular dynamics simulations, Modelling and Simulation in Materials Science and Engineering, 26 (2018) 025007.
[7] K. Oh, X.C. Zeng, Formation free energy of clusters in vapor-liquid nucleation: A Monte Carlo simulation study, The Journal of chemical physics, 110 (1999) 4471-4476.
[8] D. Srolovitz, G. Grest, M. Anderson, Computer simulation of recrystallization—I. Homogeneous nucleation and growth, Acta metallurgica, 34 (1986) 1833-1845.
[9] B. Böttger, J. Eiken, I. Steinbach, Phase field simulation of equiaxed solidification in technical alloys, Acta materialia, 54 (2006) 2697-2704.
[10] L. Gránásy, T. Börzsönyi, T. Pusztai, Nucleation and bulk crystallization in binary phase field theory, Physical review letters, 88 (2002) 206105.

[11] L. Gránásy, T. Pusztai, D. Saylor, J.A. Warren, Phase field theory of heterogeneous crystal nucleation, Physical review letters, 98 (2007) 035703.
[12] S. Wang, M. Asle Zaeem, M.F. Horstemeyer, P.T. Wang, Investigating thermal effects on morphological evolution during crystallisation of hcp metals: three-dimensional phase field study AU - Wang, S, Materials Technology, 27 (2012) 355-363.
[13] M. Asle Zaeem, H. Yin, S.D. Felicelli, Modeling dendritic solidification of Al–3%Cu using cellular automaton and phase-field methods, Applied Mathematical Modelling, 37 (2013) 3495-3503.
[14] L. Liu, S. Pian, Z. Zhang, Y. Bao, R. Li, H. Chen, A cellular automaton-lattice Boltzmann method for modeling growth and settlement of the dendrites for Al-4.7% Cu solidification, Computational Materials Science, 146 (2018) 9-17.
[15] M. Asle Zaeem, H. Yin, S.D. Felicelli, Comparison of Cellular Automaton and Phase Field Models to Simulate Dendrite Growth in Hexagonal Crystals, Journal of Materials Science & Technology, 28 (2012) 137-146.
[16] D.W. Oxtoby, Homogeneous nucleation: theory and experiment, Journal of Physics: Condensed Matter, 4 (1992) 7627.
[17] M.E. McKenzie, J.C. Mauro, Hybrid Monte Carlo technique for modeling of crystal nucleation and application to lithium disilicate glass-ceramics, Computational Materials Science, 149 (2018) 202-207.
[18] J.R. Espinosa, C. Vega, C. Valeriani, E. Sanz, Seeding approach to crystal nucleation, The Journal of Chemical Physics, 144 (2016) 034501.
[19] A. Jokisaari, C. Permann, K. Thornton, A nucleation algorithm for the coupled conserved–nonconserved phase field model, Computational Materials Science, 112 (2016) 128-138.
[20] Y. Lin, Y.-X. Liu, M.-S. Chen, M.-H. Huang, X. Ma, Z.-L. Long, Study of static recrystallization behavior in hot deformed Ni-based superalloy using cellular automaton model, Materials & Design, 99 (2016) 107-114.
[21] R.S. Aga, J.R. Morris, J.J. Hoyt, M. Mendelev, Quantitative parameter-free prediction of simulated crystal-nucleation times, Physical review letters, 96 (2006) 245701.
[22] F.H. Streitz, J.N. Glosli, M.V. Patel, Beyond finite-size scaling in solidification simulations, Physical review letters, 96 (2006) 225701.
[23] M. Descamps, J.-F. Willart, Scaling laws and size effects for amorphous crystallization kinetics: Constraints imposed by nucleation and growth specificities, International Journal of Pharmaceutics, 542 (2018) 186-195.
[24] T. Koishi, K. Yasuoka, T. Ebisuzaki, Large scale molecular dynamics simulation of nucleation in supercooled NaCl, The Journal of chemical physics, 119 (2003) 11298-11305.
[25] Y. Shibuta, S. Sakane, T. Takaki, M. Ohno, Submicrometer-scale molecular dynamics simulation of nucleation and solidification from undercooled melt: linkage between empirical interpretation and atomistic nature, Acta Materialia, 105 (2016) 328-337.
[26] Y. Shibuta, S. Sakane, E. Miyoshi, S. Okita, T. Takaki, M. Ohno, Heterogeneity in homogeneous nucleation from billion-atom molecular dynamics simulation of solidification of pure metal, Nature Communications, 8 (2017) 10.
[27] B. O'malley, I. Snook, Crystal nucleation in the hard sphere system, Physical review letters, 90 (2003) 085702.
[28] J. Wedekind, D. Reguera, R. Strey, Finite-size effects in simulations of nucleation, The Journal of chemical physics, 125 (2006) 214505.
[29] P. Rein ten Wolde, M.J. Ruiz-Montero, D. Frenkel, Numerical calculation of the rate of crystal nucleation in a Lennard-Jones system at moderate undercooling, The Journal of chemical physics, 104 (1996) 9932-9947.
[30] P.R. Ten Wolde, M.J. Ruiz-Montero, D. Frenkel, Numerical evidence for bcc ordering at the surface of a critical fcc nucleus, Physical review letters, 75 (1995) 2714.

[31] M.S. Watanabe, Percolation with a periodic boundary condition: The effect of system size for crystallization in molecular dynamics, Physical Review E, 51 (1995) 3945.
[32] J. Lutsko, D. Wolf, S. Phillpot, S. Yip, Molecular-dynamics study of lattice-defect-nucleated melting in metals using an embedded-atom-method potential, Physical Review B, 40 (1989) 2841.
[33] D. Sun, M. Mendelev, C. Becker, K. Kudin, T. Haxhimali, M. Asta, J. Hoyt, A. Karma, D. Srolovitz, Crystal-melt interfacial free energies in hcp metals: A molecular dynamics study of Mg, Physical Review B, 73 (2006) 024116.
[34] G. Díaz Leines, R. Drautz, J. Rogal, Atomistic insight into the non-classical nucleation mechanism during solidification in Ni, The Journal of chemical physics, 146 (2017) 154702.
[35] B.-J. Lee, M. Baskes, Second nearest-neighbor modified embedded-atom-method potential, Physical Review B, 62 (2000) 8564.
[36] L. Xiong, F. Guo, X. Wang, Q. Cao, D. Zhang, Y. Ren, J. Jiang, Structural evolution and dynamical properties of Al2Ag and Al2Cu liquids studied by experiments and ab initio molecular dynamics simulations, Journal of Non-Crystalline Solids, 459 (2017) 160-168.
[37] S. Sohn, Y. Jung, Y. Xie, C. Osuji, J. Schroers, J.J. Cha, Nanoscale size effects in crystallization of metallic glass nanorods, Nature communications, 6 (2015) 8157.
[38] Y. Lü, X. Zhang, M. Chen, Size Effect on nucleation rate for homogeneous crystallization of nanoscale water film, The Journal of Physical Chemistry B, 117 (2013) 10241-10249.
[39] A. Statt, P. Virnau, K. Binder, Finite-size effects on liquid-solid phase coexistence and the estimation of crystal nucleation barriers, Physical review letters, 114 (2015) 026101.
[40] M. Parrinello, A. Rahman, Polymorphic transitions in single crystals: A new molecular dynamics method, Journal of Applied physics, 52 (1981) 7182-7190.
[41] S. Plimpton, Fast parallel algorithms for short-range molecular dynamics, Journal of computational physics, 117 (1995) 1-19.
[42] A. Stukowski, Visualization and analysis of atomistic simulation data with OVITO–the Open Visualization Tool, Modelling and Simulation in Materials Science and Engineering, 18 (2009) 015012.
[43] H. Tsuzuki, P.S. Branicio, J.P. Rino, Structural characterization of deformed crystals by analysis of common atomic neighborhood, Computer physics communications, 177 (2007) 518-523.
[44] A.J. Cao, Y.G. Wei, Formation of fivefold deformation twins in nanocrystalline face-centered-cubic copper based on molecular dynamics simulations, Applied Physics Letters, 89 (2006) 041919.
[45] A. Sutton, J. Chen, Long-range finnis–sinclair potentials, Philosophical Magazine Letters, 61 (1990) 139-146.
[46] M. Finnis, J. Sinclair, A simple empirical N-body potential for transition metals, Philosophical Magazine A, 50 (1984) 45-55.
[47] S. Foiles, M. Baskes, M.S. Daw, Embedded-atom-method functions for the fcc metals Cu, Ag, Au, Ni, Pd, Pt, and their alloys, Physical review B, 33 (1986) 7983.
[48] E. Asadi, M. Asle Zaeem, S. Nouranian, M.I. Baskes, Two-phase solid–liquid coexistence of Ni, Cu, and Al by molecular dynamics simulations using the modified embedded-atom method, Acta Materialia, 86 (2015) 169-181.
[49] E. Asadi, M. Asle Zaeem, S. Nouranian, M.I. Baskes, Quantitative modeling of the equilibration of two-phase solid-liquid Fe by atomistic simulations on diffusive time scales, Physical Review B, 91 (2015) 024105.
[50] E. Asadi, M. Asle Zaeem, The anisotropy of hexagonal close-packed and liquid interface free energy using molecular dynamics simulations based on modified embedded-atom method, Acta Materialia, 107 (2016) 337-344.
[51] X. Dai, Y. Kong, J. Li, B. Liu, Extended Finnis–Sinclair potential for bcc and fcc metals and alloys, Journal of Physics: Condensed Matter, 18 (2006) 4527.

[52] M.S. Daw, S.M. Foiles, M.I. Baskes, The embedded-atom method: a review of theory and applications, Materials Science Reports, 9 (1993) 251-310.
[53] D.Y. Sun, M.I. Mendelev, C.A. Becker, K. Kudin, T. Haxhimali, M. Asta, J.J. Hoyt, A. Karma, D.J. Srolovitz, Crystal-melt interfacial free energies in hcp metals: A molecular dynamics study of Mg, Physical Review B, 73 (2006) 024116.
[54] Y.-M. Kim, N.J. Kim, B.-J. Lee, Atomistic modeling of pure Mg and Mg–Al systems, Calphad, 33 (2009) 650-657.
[55] G. Simmons, H. Wang, Single crystal elastic constants and calculated aggregate properties, (1971).
[56] W.F. Gale, T.C. Totemeier, Smithells metals reference book, Butterworth-Heinemann, 2003.
[57] A.M. James, M.P. Lord, Macmillan's chemical and physical data, Macmillan, 1992.
[58] J.G. Speight, Lange's handbook of chemistry, McGraw-Hill New York, 2005.
[59] Q. Jiang, H. Lu, Size dependent interface energy and its applications, Surface Science Reports, 63 (2008) 427-464.
[60] L. Gránásy, M. Tegze, A. Ludwig, Solid–liquid interfacial free energy, in: Rapidly Quenched Materials, Elsevier, 1991, pp. 577-580.
[61] M. Gündüz, J. Hunt, The measurement of solid-liquid surface energies in the Al-Cu, Al-Si and Pb-Sn systems, Acta Metallurgica, 33 (1985) 1651-1672.
[62] M.S. Daw, M.I. Baskes, Embedded-atom method: Derivation and application to impurities, surfaces, and other defects in metals, Physical Review B, 29 (1984) 6443.
[63] R. Boehler, Temperatures in the Earth's core from melting-point measurements of iron at high static pressures, Nature, 363 (1993) 534.
[64] L. Swartzendruber, Melting point of iron, Journal of Phase Equilibria, 5 (1984) 339-339.
[65] J. Liu, R. Davidchack, H. Dong, Molecular dynamics calculation of solid–liquid interfacial free energy and its anisotropy during iron solidification, Computational Materials Science, 74 (2013) 92-100.
[66] E. Brandes, G. B (Editors), Smithells Metals Reference Book, Butter worth, in, Heinemann, Oxford, 1992.
[67] J.B. Enns, J.K. Gillham, Time–temperature–transformation (TTT) cure diagram: Modeling the cure behavior of thermosets, Journal of Applied Polymer Science, 28 (1983) 2567-2591.
[68] Y. Shibuta, K. Oguchi, T. Takaki, M. Ohno, Homogeneous nucleation and microstructure evolution in million-atom molecular dynamics simulation, Scientific Reports, 5 (2015) 13534.
[69] S. Nosé, A molecular dynamics method for simulations in the canonical ensemble, Molecular physics, 52 (1984) 255-268.
[70] A. Di Cicco, A. Trapananti, S. Faggioni, A. Filipponi, Is there icosahedral ordering in liquid and undercooled metals?, Physical review letters, 91 (2003) 135505.
[71] G. Kikugawa, S. Ando, J. Suzuki, Y. Naruke, T. Nakano, T. Ohara, Effect of the computational domain size and shape on the self-diffusion coefficient in a Lennard-Jones liquid, The Journal of chemical physics, 142 (2015) 024503.
[72] I.-C. Yeh, G. Hummer, System-size dependence of diffusion coefficients and viscosities from molecular dynamics simulations with periodic boundary conditions, The Journal of Physical Chemistry B, 108 (2004) 15873-15879.
[73] N. Volkov, M. Posysoev, A. Shchekin, The Effect of Simulation Cell Size on the Diffusion Coefficient of an Ionic Surfactant Aggregate, Colloid Journal, 80 (2018) 248-254.
[74] J. Wedekind, D. Reguera, What is the best definition of a liquid cluster at the molecular scale?, The Journal of chemical physics, 127 (2007) 154516.
[75] J. Wedekind, D. Reguera, Kinetic reconstruction of the free-energy landscape, The Journal of Physical Chemistry B, 112 (2008) 11060-11063.
[76] H. Risken, Fokker-planck equation, in: The Fokker-Planck Equation, Springer, 1996, pp. 63-95.

[77] S. An, J. Li, Y. Li, S. Li, Q. Wang, B. Liu, Two-step crystal growth mechanism during crystallization of an undercooled Ni 50 Al 50 alloy, Scientific reports, 6 (2016) 31062.
[78] C. Li, R. Tao, S. Luo, X. Gao, K. Zhang, Z. Li, Enhancing and Impeding Heterogeneous Ice Nucleation through Nanogrooves, The Journal of Physical Chemistry C, 122 (2018) 25992-25998.